PHYSICAL REVIEW B **83**, 161103(R) (2011)

Incorporating dynamic mean-field theory into diagrammatic Monte Carlo

Lode Pollet,[1] Nikolay V. Prokof'ev,[2,3] and Boris V. Svistunov[2,3]
[1]*Theoretische Physik, ETH Zurich, 8093 Zurich, Switzerland*
[2]*Department of Physics, University of Massachusetts, Amherst, Massachusetts 01003, USA*
[3]*Russian Research Center "Kurchatov Institute," 123182 Moscow, Russia*
(Received 7 March 2011; published 20 April 2011)

The bold diagrammatic Monte Carlo (BDMC) method performs an unbiased sampling of Feynman's diagrammatic series using skeleton diagrams. For lattice models the efficiency of BDMC can be dramatically improved by incorporating dynamical mean-field theory (DMFT) solutions into renormalized propagators. From the DMFT perspective, combining it with BDMC leads to an unbiased method with well-defined accuracy. We illustrate the power of this approach by computing the single-particle propagator (and thus the density of states) in the non-perturbative regime of the Anderson localization problem, where a gain of the order of 10^4 is achieved with respect to conventional BDMC in terms of convergence to the exact answer.

DOI: 10.1103/PhysRevB.83.161103 PACS number(s): 05.10.Ln, 02.70.Ss

A skeleton diagrammatic series is nothing but Feynman's diagrammatic expansion in terms of "dressed" or "bold-line" propagators, interaction lines, and vertices, which account for the summation of certain subclasses of diagrams. Its power lies in the fact that, even when truncated to the lowest orders, it often captures the basic physics of strongly correlated systems and yields quantitatively accurate answers. Among its numerous successes we mention screening effects, self-consistent Hartree-Fock schemes, the GW approximation for simple metals, Bogoliubov and Gor'kov-Nambu equations, and so on. Often, as, e.g., in case of Kohn-Sham orbitals in density functional theory, the diagrammatic structure is hidden in a set of integral equations, whose implementation has been improved to perfection. Physically, the lowest-order skeleton graphs embody the idea of incorporating some "mean-field" theory self-consistently.

The main shortcoming of self-consistent treatments based on the lowest-order diagrams is lack of accuracy and control: the error due to truncation can be established only by reliably calculating contributions of higher-order diagrams, which in the typical case of optimized codes solving a set of self-consistent integral equations is nearly impossible. Moreover, in the absence of small parameters order of magnitude estimates are essentially meaningless. The recently developed bold diagrammatic Monte Carlo (BDMC) method[1] allows one to sample skeleton Feynman expansions far beyond the mean-field level. Given that even the diagrammatic Monte Carlo method based on bare propagators can produce very accurate results for correlated systems (say, for the repulsive fermionic Hubbard model[2,3]), BDMC emerges as a powerful generic field-theoretical method. It has been successfully applied to the fermi-polaron problem[1] and, very recently, determined the equation of state in a system of resonant fermions.[4] The above examples deal with continuous-space problems, but it is natural to expect that working with the skeleton series will bring significant advantages to lattice models as well.

Here, we show that, in addition to going from a bare to a skeleton expansion, a dramatic increase in performance can be reached by employing an exact series resummation procedure, which sums up all local contributions to the self-energy. This approach is tantamount to embedding the dynamical mean-field theory (DMFT)[5] solution into an exact diagrammatic method and avoids any double counting or other uncontrollable errors. The gain in efficiency comes from two related observations: an impressive success of DMFT applications[5–7] and the fact that the summation of local contributions can be done separately by a variety of highly efficient methods. The BDMC + DMFT approach thus involves two distinct but cross-linked numerical processes: (i) a problem-specific solver of the DMFT-type problem (to be referred to as "impurity solver," in accordance with terminology accepted in literature) and (ii) a generic BDMC scheme simulating skeleton diagrams which cannot be reduced to the purely local ones. The protocol is illustrated in Fig. 1.

Below we start with the precise formulation of the combined scheme and then proceed with its implementation for finding a disorder-averaged single-particle propagator (and thus the density of states) in the nonperturbative regime of Anderson localization, which is well suited for illustrating the idea because the efficiency gained by incorporating DMFT solutions within BDMC is about 10^4. We stress that our goal in this Rapid Communication is to explain the new method and illustrate its implementation, not to solve the localization problem in its full complexity. In general, the gain will be problem and parameter specific, and will also depend on the efficiency of the impurity solver. Nevertheless, there is a general argument why using the DMFT-based method (or any other method more efficient than DMFT) of summing the local diagrams must yield an efficiency gain in cases when DMFT captures the leading contribution: In view of the (asymptotically) factorial complexity of BDMC, the computation time depends dramatically on the desired error bar. A desired error bar of 1% requires an order of magnitude longer simulation time than a desired error bar of 3%. Now if, say, 90% of the answer is captured by some efficient method which is *compatible with diagrammatics*[8] and we are aiming at, say, an accuracy of 1% in the final answer, the BDMC simulation of the residual diagrammatic series (contributing only 10% of the answer) can be done with a relative accuracy of 10%. We note that other resummation techniques, as, for instance, developed for the nonlinear σ model in the large N limit,[9] may also be worthwhile.

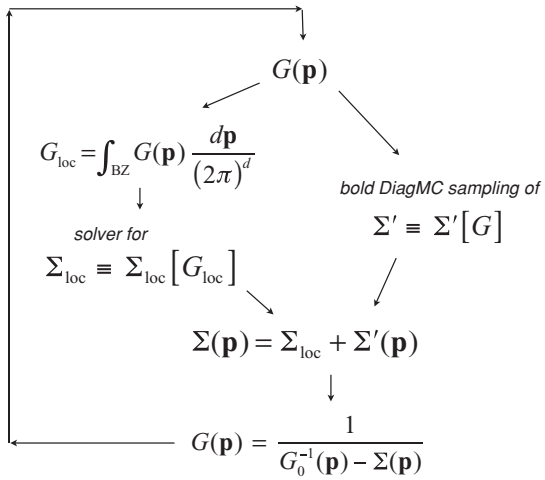

FIG. 1. Schematic representation of the BDMC + DMFT protocol (see text for the details).

The protocol of reformulating skeleton series to account for all local contributions to self-energy is conceptually straightforward. The Dyson equation relates the Green's function, G, to the self-energy, Σ (for clarity, we suppress below the frequency variable):

$$G(\mathbf{p}) = \frac{1}{G_0^{-1}(\mathbf{p}) - \Sigma(\mathbf{p})}, \tag{1}$$

with G_0 standing for the nonperturbed Green's function. The local propagator $G_{\rm loc}$ is defined by integrating over the Brillouin zone (BZ):

$$G_{\rm loc} = \int_{\rm BZ} G(\mathbf{p}) \frac{d\mathbf{p}}{(2\pi)^d}. \tag{2}$$

We now separate contributions to the self-energy into two parts

$$\Sigma(\mathbf{p}) = \Sigma_{\rm loc} + \Sigma'(\mathbf{p}), \tag{3}$$

where $\Sigma_{\rm loc}$ is given by irreducible skeleton diagrams which involve *exclusively* $G_{\rm loc}$ propagators. In other words, this local propagator has only purely momentum independent building blocks, while all the rest is put in Σ'.

Numerically, one calculates the self-energy using current knowledge of the Green's function and then uses it to permanently improve the knowledge of G within the self-consistent process. This involves two steps. First, the current knowledge of $G_{\rm loc}$ serves as an input for the calculation of $\Sigma_{\rm loc} \equiv \Sigma_{\rm loc}[G_{\rm loc}]$ achieved by the impurity solver, and $G(\mathbf{p})$ is used for the BDMC simulation of the remaining skeleton graphs. Second, self-energies $\Sigma_{\rm loc}$ and Σ' are combined into the total self-energy, Eq. (3), which is then used to find the updated G by Eq. (1). This is illustrated in Fig. 1.

Technically, the crucial advantage of separating local contributions to the self-energy is that the corresponding momentum-independent problem admits a variety of techniques for solving it very efficiently.[10] Treating the local physics nonperturbatively is very appealing from the physical viewpoint. In typical problems such as the Hubbard model, the diagrammatic technique expands around the noninteracting limit which is dominated by large hopping processes. The competing phase with large on-site interactions tends on the contrary to localize the particles. Hence, building diagrams on top of the solution capturing essential physics of the competing phase may be better suited for describing the difficult intermediate regime as well. Local physics is also dominant at high temperatures which can easily be understood in terms of Feynman's path integrals.

From Eqs. (1)–(2) it is explicitly seen that the BDMC + DMFT process builds an *exact* solution of the problem on top of the DMFT answer, which is crucial not only for improving the quality of the final result but also for obtaining reliable estimates of corrections to mean-field results.

One of the solvers for obtaining $\Sigma_{\rm loc}$ in terms of $G_{\rm loc}$ widely used in the standard DMFT approach is based on an *implicit* formulation of the problem in terms of the single-site (or impurity) effective action with a certain auxiliary (to be determined) "bare" propagator $\tilde{g}_0$. The advantage of this formulation is in the flexibility of designing efficient tools (impurity solvers)[10] for evaluating $Q[\tilde{g}_0]$, where Q stands for the operator converting the bare propagator into the corresponding Green's function. The process of obtaining $\Sigma_{\rm loc}[G_{\rm loc}]$ amounts then to finding $\tilde{g}_0$ satisfying the equation

$$Q[\tilde{g}_0] = G_{\rm loc} \tag{4}$$

(this can be done by appropriately iterating $\tilde{g}_0$) and using $\Sigma_{\rm loc} = \tilde{g}_0^{-1} - G_{\rm loc}^{-1}$. Solvers based on the effective action approach play a crucial part when the diagrammatic expansion of $\Sigma_{\rm loc}[G_{\rm loc}]$ cannot be used because of technical or convergence problems.

We illustrate the introduced concepts for Anderson's model of particle localization on a disordered three-dimensional cubic lattice. We consider δ-correlated Gaussian disorder in the chemical potential, for which the standard diagrammatic technique can be formulated.[11] The Hamiltonian, in standard lattice notation, reads

$$H = -J \sum_{\langle i,j \rangle} \hat{c}_i^\dagger \hat{c}_j + \sum_i \epsilon_i \hat{n}_i . \tag{5}$$

The random on-site potential ϵ_i is distributed with the Gaussian probability density

$$P(\epsilon) = \frac{e^{-\epsilon^2/2V^2}}{\sqrt{2\pi V^2}}, \tag{6}$$

with the dispersion V characterizing the strength of disorder. We choose J as an energy unit. We work in the real-space and real-time representation where the Green function is defined as $G(\mathbf{r},t'-t) = -i \langle \mathcal{T} c(0,t)\, c^\dagger(\mathbf{r},t') \rangle$ and consider a lattice of size $12 \times 12 \times 12$ for checking against the exact diagonalization results, see Refs. 12 and 13. Just like in conventional DMFT larger lattices pose no problem at all; in fact, they would suppress revivals and hence make the simulations faster. The (local) density of states is given by the imaginary part of the Fourier transform $\mathrm{DOS}(\omega) = -\pi^{-1}\mathrm{Im}G(\mathbf{r}=0,\omega)$.

Evaluating the sum of all skeleton diagrams involving local propagators only (i.e., the DMFT part[14]) simplifies for Anderson localization since disorder lines have no time dependence. For a single-site problem, before averaging over disorder, the Green's function in the frequency representation

equals $1/[1/\tilde{g}_0(\omega) - i\epsilon]$. Averaging over disorder amounts to performing a simple one-dimensional integral:

$$G_{\rm loc}(\omega) = \frac{\tilde{g}_0(\omega)}{\sqrt{2\pi V^2}} \int \frac{e^{-\epsilon^2/2V^2}}{1 - i\epsilon\tilde{g}_0(\omega)}\, d\epsilon \ . \qquad (7)$$

The local self-energy then follows from $\Sigma_{\rm loc}(\omega) = \tilde{g}_0^{-1}(\omega) - G_{\rm loc}^{-1}(\omega)$ which accounts for the implicit (parametric) complex-number relation $\Sigma_{\rm loc}[G_{\rm loc}]$, i.e., the goal is achieved by the semianalytic exact solution. In practice this is done by a parametrization of the above integral equation through $\tilde{g}_0[G_{\rm loc}]$ (inversion) and iterating until self-consistency is reached, which works fine because the interaction lines carry no time dependence. In Fig. 2 we show for various disorder strengths the local self-energy obtained for $\Sigma' = 0$ after convergence, i.e., the answer as predicted by the conventional DMFT approach.

The full calculation involves Monte Carlo sampling of all skeleton diagrams except those contributing to $\Sigma_{\rm loc}$ (which would otherwise dominate in the final answer already for $V = \sqrt{2}$). In the real-space representation this means that only skeleton graphs which contain at least two vertices with different site indices are accounted for in Σ'. The simulation itself was done using standard BDMC rules with the self-consistency loop implemented exactly as described in the introductory part. It turns out that the diagrammatic series for Anderson localization constitutes the "worst case scenario" in terms of convergence properties. Although for any finite time t the series are convergent [allowing us to use Dyson's equation and Eq. (7)], the required expansion order increases dramatically with time t. Realistically, we were able to deal with skeleton graphs up to order $n_{\rm max} \sim 50$ which was limiting the accessible times in the simulation of Σ'. We observe that the values of $\Sigma'_{\mathbf{r}-\mathbf{r}'} \equiv \Sigma'_{\mathbf{n}}$ turn out to be extremely small, about two orders of magnitude smaller than $\Sigma_{\rm loc}$ even in the intermediate coupling regime $V = \sqrt{2}$, see Fig. 3. Since the complexity, and hence the *relative* error bar, of the BDMC simulation turns out to be roughly the same for simulating Σ or Σ', we conclude that the BDMC + DMFT scheme produces results which are two orders of magnitude more accurate for the same simulation time (or a speedup of $\sim 10^4$ for the same error bar). This constitutes the proof of principle for the proposed scheme. Final results for the density of states are indistinguishable from the exact diagonalization data. Our protocol allowed for calculations for $V^2 = 0.5$ up to time $t = 8$ and for $V^2 = 4$ to time $t = 3$ with similar effort and accuracy as for our demonstration parameters $V^2 = 2$ to time $t = 3$.

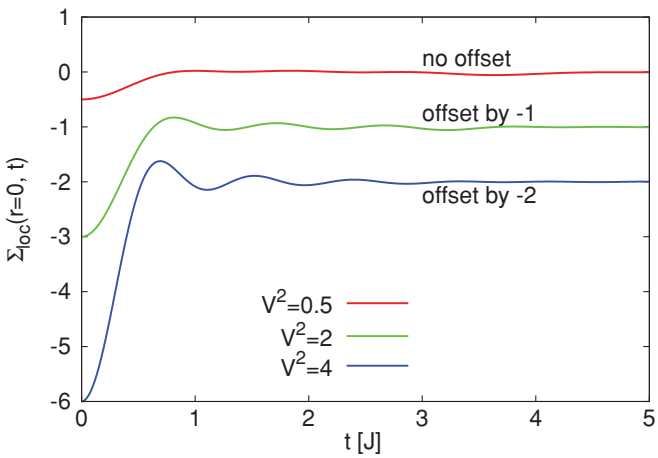

FIG. 2. (Color online) Local self-energy calculated with local propagators ($\Sigma' = 0$) for disorder strengths $V = 1/\sqrt{2}, \sqrt{2}, 4$ on a lattice of size $12 \times 12 \times 12$.

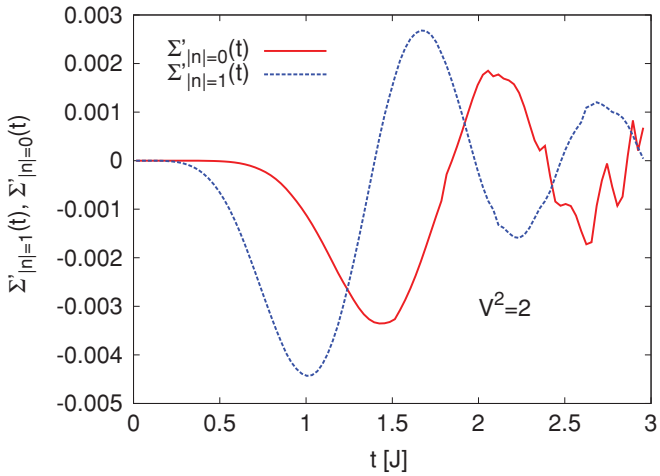

FIG. 3. (Color online) Correction to local self-energy for $V = \sqrt{2}$ on a lattice of size $12 \times 12 \times 12$: $\Sigma'_{|\mathbf{n}|=0}(t)$ (red solid line) and $\Sigma'_{|\mathbf{n}|=1}(t)$ (blue dashed line). The noise in the curve is indicative of the error bars. The sign problem and the high expansion orders put a limit on the accessible times.

In conclusion, we have introduced an approach that uses DMFT as an integral part of performing simulations of skeleton graphs in strongly interacting systems. It combines the power of solving impurity problems efficiently with an unbiased and exact diagrammatic formalism. The very close agreement between DMFT and diagrammatic Monte Carlo with bare propagators, which was explicitly demonstrated for the Hubbard model at $U/J = 4$[3], ensures that the present formalism will bring radical speed up and accuracy gains to studies of the Hubbard model and allow them to be performed at larger values of U and lower temperatures, for which new methods are still clearly needed: although several extensions to DMFT have been proposed,[6,7,10,15] controlled accuracy can, e.g., in the state-of-the-art case of cluster-DMFT for the $3d$ Hubbard model, be guaranteed only for roughly $U < 12t$ and temperatures of the order of the Néel temperature[16] with a maximum cluster size of about 100.[17]

We would also like to mention several generalizations of the simplest scheme introduced above. To begin with, the definition of momentum-independent propagator allows to use an arbitrary function $f(\mathbf{p})$ in the definition of $G_{\rm loc}$ such that $G_{\rm loc} = \int_{\rm BZ} G(\mathbf{p}) f(\mathbf{p})\, d\mathbf{p}/(2\pi)^d$. The rest of the scheme remains intact: As before, diagrams *exclusively* containing $G_{\rm loc}$ propagators are all summed up in the local self-energy, while Σ' contains at least one line which is based on $G(\mathbf{p}) - G_{\rm loc}$. The freedom of choosing $f(\mathbf{p})$ that differs from a constant may be used to optimize the subtraction of leading terms.

In the generic many-body skeleton diagram, any renormalized line whether it is the single-particle propagator, $G(\mathbf{p})$, the

interaction line, $W(\mathbf{q})$, or the two-particle propagator, Γ, can be split into momentum-independent and momentum-dependent parts (with the same freedom of defining the local part as described in the previous paragraph). Next, all diagrams based *exclusively* on momentum-independent lines can be dealt with using impurity solvers with BDMC accounting for the remaining graphs. Since the summation of certain geometric series such as ladder or screening diagrams can be done analytically, one can go even beyond the purely local physics.

Our final remark is that nothing prevents one from extending the idea of subtracting diagrams with momentum-independent lines (and compensating them separately by impurity solvers) to subtracting diagrams with specific momentum-dependence and structure (and compensating them by impurity solvers dealing with a few sites, similarly to the ideas behind cluster-DMFT schemes). The diagrams to be summed up by the impurity solver are those with the connections of a compact cluster of sites. Similar extensions for real-space clusters are also possible.

The authors are grateful to A. Georges, E. Gull, P. Werner, and M. Troyer for useful discussions. This work was supported by the National Science Foundation Grant No. PHY-1005543, the Swiss National Science Foundation under Grant No. PZ00P2-131892/1, and by a grant from the Army Research Office with funding from the DARPA OLE program. We thank the Aspen Center of Physics, KITP Santa Barbara, and Casa Física at UMass for hospitality. Simulations were performed on the Brutus cluster at ETH Zurich and CM cluster at UMass, Amherst.

[1] N. V. Prokof'ev and B. V. Svistunov, Phys. Rev. Lett. **99**, 250201 (2007); Phys. Rev. B **77**, 125101 (2008).

[2] K. Van Houcke, E. Kozik, N. Prokof'ev, and B. Svistunov, in *Computer Simulation Studies in Condensed Matter Physics XXI*, edited by D. P. Landau, S. P. Lewis, and H. B. Schuttler (Springer Verlag, Berlin, 2008).

[3] E. Kozik, K. Van Houcke, E. Gull, L. Pollet, N. Prokof'ev, B. Svistunov, and M. Troyer, Europhys. Lett. **90**, 10004 (2010).

[4] K. Van Houcke *et al*. (in preparation).

[5] A. Georges, G. Kotliar, W. Krauth, and M. J. Rozenberg, Rev. Mod. Phys. **68**, 13 (1996).

[6] G. Kotliar, S. Y. Savrasov, K. Haule, V. S. Oudovenko, O. Parcollet, and C. A. Marianetti, Rev. Mod. Phys. **78**, 865 (2006).

[7] T. Maier, M. Jarrell, T. Pruschke, and M. H. Hettler, Rev. Mod. Phys. **77**, 1027 (2005).

[8] By compatibility with diagrammatics we mean the possibility of expressing the residual contributions in terms of (skeleton) diagrammatic expansions without approximations and double counting—a crucial requirement for the combined method to remain unbiased.

[9] P. V. Buividovich, Phys. Rev. D **83**, 045021 (2011).

[10] E. Gull, A. J. Millis, A. I. Lichtenstein, A. N. Rubtsov, M. Troyer, and P. Werner, e-print arXiv:1012.4474, to appear in Rev. Mod. Phys. (2010).

[11] A. A. Abrikosov, L. P. Gor'kov, and I. E. Dzyaloshinski, *Methods of Quantum Field Theory in Statistical Physics*, (Dover, Mineola, NY, 1975).

[12] M. V. Feigel'man, L. B. Ioffe, V. E. Kravtsov, and E. Cuevas, Ann. Phys. **325**, 1390 (2010).

[13] N. C. Murphy, R. Wortis, and W. A. Atkinson, e-print arXiv:1011.0659 (2010).

[14] K. Byczuk, W. Hofstetter, and D. Vollhardt, in *50 Years of Anderson Localization*, edited by E. Abrahams (World Scientific, Singapore, 2010), p. 473; reprinted in Int. J. Mod. Phys. B **24**, 1727 (2010).

[15] A. N. Rubtsov, M. I. Katsnelson, and A. I. Lichtenstein, Phys. Rev. B **77**, 033101 (2008).

[16] S. Fuchs, E. Gull, L. Pollet, E. Burovski, E. Kozik, T. Pruschke, and M. Troyer, Phys. Rev. Lett. **106**, 030401 (2011).

[17] E. Gull, P. Staar, S. Fuchs, P. Nukala, M. S. Summers, T. Pruschke, T. C. Schulthess, and T. Maier, Phys. Rev. B **83**, 075122 (2011).